Vitamin E does not prevent Western diet-induced NASH progression and increases metabolic flux dysregulation in mice

Clinton M. Hasenour,* Arion J. Kennedy,[†] Tomasz Bednarski,* Irina A. Trenary,* Brandon J. Eudy,[§] Robin P. da Silva,[§] Kelli L. Boyd,** and Jamey D. Young[1,*,†,††]

Departments of Chemical and Biomolecular Engineering,* Molecular Physiology and Biophysics,[†] and Pathology, Microbiology, and Immunology,** and Mouse Metabolic Phenotyping Center,[††] Vanderbilt University, Nashville, TN; and Department of Food Science and Human Nutrition,[§] University of Florida, Gainesville, FL

ORCID ID: 0000-0002-0871-1494 (J.D.Y.)

Abstract Fatty liver involves ectopic lipid accumulation and dysregulated hepatic oxidative metabolism, which can progress to a state of elevated inflammation and fibrosis referred to as nonalcoholic steatohepatitis (NASH). The factors that control progression from simple steatosis to NASH are not fully known. Here, we tested the hypothesis that dietary vitamin E (VitE) supplementation would prevent NASH progression and associated metabolic alterations induced by a Western diet (WD). Hyperphagic melanocortin-4 receptor-deficient (MC4R$^{-/-}$) mice were fed chow, chow+VitE, WD, or WD+VitE starting at 8 or 20 weeks of age. All groups exhibited extensive hepatic steatosis by the end of the study (28 weeks of age). WD feeding exacerbated liver disease severity without inducing proportional changes in liver triglycerides. Eight weeks of WD accelerated liver pyruvate cycling, and 20 weeks of WD extensively upregulated liver glucose and oxidative metabolism assessed by ^{2}H/^{13}C flux analysis. VitE supplementation failed to reduce the histological features of NASH. Rather, WD+VitE increased the abundance and saturation of liver ceramides and accelerated metabolic flux dysregulation compared with 8 weeks of WD alone. **JLR** In summary, VitE did not limit NASH pathogenesis in genetically obese mice, but instead increased some indicators of metabolic dysfunction.—Hasenour, C. M., A. J. Kennedy, T. Bednarski, I. A. Trenary, B. J. Eudy, R. P. da Silva, K. L. Boyd, and J. D. Young. **Vitamin E does not prevent Western diet-induced NASH progression and increases metabolic flux dysregulation in mice.** *J. Lipid Res.* 2020. 61: 707–721.

Metabolic disease is plaguing millions of US citizens and has placed a heavy financial burden on the US healthcare system. One such pathology is nonalcoholic fatty liver disease (NAFLD), the hepatic manifestation of metabolic syndrome. NAFLD is a spectrum disorder that ranges from simple steatosis to nonalcoholic steatohepatitis (NASH), a state of heightened liver inflammation, cellular injury, and fibrosis (1). The National Institutes of Health report that 30–40% of US adults have NAFLD and 3–12% suffer from NASH, conditions which track with insulin resistance and increase the risk of cirrhosis, liver cancer, and cardiovascular disease. Despite its significance, the underlying molecular mechanisms that control NAFLD progression to NASH remain poorly understood, and there are currently no FDA-approved pharmacotherapies for NAFLD or NASH.

Mitochondrial dysregulation is a core feature of NAFLD. Recent work has implemented isotope-based flux analysis to probe liver mitochondrial metabolism and its linkage to

Abbreviations: ALT, alanine transaminase; AST, aspartate transaminase; BHB, β-hydroxybutyrate; CAC, citric acid cycle; FID, flame ionization detector; HFF, high-fat feeding; LDH, lactate dehydrogenase; MC4R$^{-/-}$, melanocortin-4 receptor-deficient; MID, mass isotopomer distribution; NAFLD, nonalcoholic fatty liver disease; NASH, nonalcoholic steatohepatitis; ROS, reactive oxygen species; TFD, high-*trans*-fat and high-fructose diet; V$_{CS}$, citric acid cycle flux; V$_{EndoRa}$, endogenous glucose production; V$_{Enol}$, gluconeogenesis from the citric acid cycle; VitE, vitamin E; V$_{LDH}$, net anaplerotic flux; V$_{PC}$, anaplerotic flux through pyruvate carboxylase; V$_{PCK}$, cataplerotic flux through phosphoenolpyruvate carboxykinase; V$_{PK+ME}$, "pyruvate cycling" through pyruvate kinase, malic enzyme, or overlapping fluxes; V$_{PYGL}$, glycogenolytic flux; WD, Western diet.

[1]To whom correspondence should be addressed.
  e-mail: j.d.young@vanderbilt.edu

glucose production in the pathogenesis of fatty liver disease (2–4). From this research, it is evident that lipid oversupply to the liver can increase citric acid cycle (CAC) activity and gluconeogenesis in vivo. A rational explanation for the latter is that products of fatty acid β-oxidation support glucose synthesis through enzymatic regulation of pyruvate carboxylation and dehydrogenation (5–10). The activation of CAC metabolism may be linked to abnormalities in liver ATP homeostasis observed in insulin resistance (11, 12) and NASH (13). In these conditions, increased energy demand, impaired β-oxidation, and/or inefficiencies in electron transport may place a greater demand on the CAC for NADH and flavin adenine dinucleotide hydroquinone ($FADH_2$) generation (2–4).

More recently, substrate-supported and uncoupled mitochondrial respiration was found to be elevated in liver biopsies from obese patients with and without NAFLD. In contrast, biopsies from patients with NASH exhibited a blunted mitochondrial respiratory response. The impairment in respiratory capacity was associated with a reduction in antioxidant defenses and increased oxidative damage, leading the authors to conclude that certain protective metabolic adaptations that occur in NAFLD are subsequently lost in NASH (14). While these results powerfully characterize the state of liver mitochondrial function in obese NAFLD and NASH patients, they do not assess how liver intermediary metabolism adapts to the progression from NAFLD to NASH when situated in the often redundant and cross-regulatory in vivo milieu. Furthermore, such comparisons can be confounded by the gradual loss of mitochondrial function that occurs due to the aging process if the study cohorts are not age-matched.

The progression from NAFLD to NASH, along with its associated metabolic dysfunction, may also be sensitive to the composition of fatty acids supplied from exogenous sources (e.g., diet composition) (15). For example, intravenous lipid infusions in rats cause an ER stress response in the liver that varies with the saturation of the lipid emulsion (16). In obese nondiabetic human subjects, enteral delivery of palm oil impairs insulin-mediated reductions in glucose production compared with safflower oil (17). These results are consistent with in vitro work demonstrating that palmitate administration increases glutamine anaplerosis, CAC activity, ER stress, and apoptosis through a Ca^{2+}-dependent mechanism (18–20), whereas coadministration of oleate rescues hepatocytes from palmitate-induced lipotoxicity and associated metabolic alterations (21). In obesity, the ER exhibits an increase in monounsaturated lipid species, a decrease in polyunsaturated lipid species, disrupted Ca^{2+} homeostasis, and increased ER stress (22). Thus, diet-induced perturbations to liver lipid composition may indirectly promote metabolic dysregulation through mechanisms involving loss of ER membrane function and Ca^{2+} handling, in addition to the direct effects of dietary lipids to supply fuel to liver mitochondria.

Overactive hepatic metabolism in response to lipid overload also associates with increased oxidative demand and accumulation of reactive oxygen species (ROS) in vitro (18, 19) and in vivo (2). In NASH, increased oxidative stress and limitations to antioxidant capacity (14) may promote liver inflammation, fibrosis, and apoptosis (23). These observations have led some to evaluate the efficacy of the antioxidant vitamin E (VitE), a lipid-soluble peroxyl-radical scavenger, in the treatment or prophylaxis of NAFLD/NASH in rodents (24–26) and humans (27, 28). The PIVENS trial (27) concluded that VitE treatment of adults without diabetes resulted in a significantly higher rate of improvement in NASH compared with placebo. However, VitE did not have similar efficacy in a recent clinical trial of patients with type 2 diabetes (29).

Given the uncertainties surrounding the role of dysregulated hepatic oxidative metabolism in promoting the progression from NAFLD to NASH, we designed a study to examine the impacts of diet composition and VitE treatment on fatty liver phenotypes using an obese mouse model that has been previously shown to rapidly and spontaneously develop characteristics of human NASH upon Western diet (WD) feeding. The studies described herein addressed three central metabolic questions in vivo: *1*) how does the overconsumption of a WD high in saturated fat, cholesterol, and sucrose impact liver lipid composition and markers of NAFLD/NASH; *2*) how does liver glucose and oxidative metabolism change in response to worsening steatotic liver disease; and *3*) are these phenotypes resolved through increased dietary supply of VitE? These questions were tested in age-matched, hyperphagic, male mice deficient in the melanocortin-4 receptor ($MC4R^{-/-}$), which are reported to develop simple steatosis when fed a standard chow diet and NASH when fed a WD (30, 31). Mice were maintained on chow or switched to WD for 8 or 20 weeks to amplify liver disease severity. Static characteristics of WD-mediated liver injury and lipid profiles were measured alongside in vivo rates of hepatic CAC, anaplerosis, and gluconeogenesis fluxes in all groups. This design allowed us to capture the impact of WD on in vivo NASH pathogenesis in the presence (WD for 20 weeks) and absence (WD for 8 weeks) of gains in body weight and adiposity. Additional cohorts of mice were fed the same diets (chow, 8 weeks WD, or 20 weeks WD) supplemented with VitE to examine whether NASH severity could be reduced through elevated dietary intake of a lipid-soluble antioxidant.

MATERIALS AND METHODS

In vivo procedures in the mouse

All procedures were performed with approval from the Vanderbilt Animal Care and Use Committee. All studies were performed on ∼28-week-old male $MC4R^{-/-}$ mice; parental breeders were generously provided by the Roger D. Cone laboratory (32). Mice were given ad libitum access to diets and water and maintained on a 12:12 h light-dark cycle in a temperature- (23°C) and humidity-stable environment. After weaning, mice were provided a standard chow diet (5L0D, 29% protein, 58% carbohydrates, 13% fat by caloric contribution; LabDiet, St. Louis, MO). At 8 weeks of age, some mice were switched to WD (D12079B, 17% protein, 43% carbohydrates, and 40% fat by caloric contribution; Research Diets Inc., New Brunswick, NJ) or WD+VitE (supplemented to 500 IU/kg dl-α-tocopherol acetate, a roughly 10-fold higher concentration

than in D12079B) for 20 weeks. Others were maintained on chow until 20 weeks of age, when they were switched to chow+VitE (5L0D supplemented to 500 IU/kg), WD, or WD+VitE for 8 weeks. Overall, six groups were utilized for the studies presented here: chow, chow+VitE (for 8 weeks), WD for 8 weeks, WD+VitE for 8 weeks, WD for 20 weeks, and WD+VitE for 20 weeks (**Fig. 1A**). Dietary VitE supplementation was based on prior measurements of food consumption reported for MC4R$^{-/-}$ mice (32); VitE intake was estimated to be ~2.5 IU/mouse/day when diets were supplemented to 500 IU/kg. Measurements of liver α-tocopherol concentrations produced by each diet are presented in Fig. 1B.

Indwelling catheters were surgically implanted in the jugular vein and carotid artery ~1 week prior to experimentation for infusing and sampling, respectively, as previously described (33). In vivo studies were performed similarly to those described in detail elsewhere in long-term-fasted (~20 h) mice, with minor modifications (34). Briefly, mice received an intravenous primed (440 μmol/kg) continuous (4.4 μmol/kg/min) infusion of [6,6-^{2}H$_2$] glucose and a bolus of ^{2}H$_2$O to enrich body water to 4.5% (abbreviated collectively as ^{2}H). Two hours later, mice received a primed (1.1 mmol/kg) continuous (0.055 mmol/kg/min) infusion of sodium [^{13}C$_3$]propionate (Cambridge Isotope Laboratories, Tewksbury, MA). Isotopes were delivered over an ~4.5 h time course, as previously described (34), and plasma glucose samples were obtained from the arterial circulation roughly 2 h after the start of the [^{13}C$_3$]propionate infusion to allow isotopic labeling to fully equilibrate. At the close of the study, mice were euthanized through cervical dislocation and liver tissue was rapidly excised and freeze-clamped in liquid nitrogen; plasma samples and tissues obtained at the end of the study were stored at −80°C prior to analysis. Additional age-matched cohorts of mice from each group were maintained similarly, except without surgery or isotope tracer infusions, for body composition, plasma, and tissue analysis following a brief (5 h) fast to assess static metrics of patho-physiology. Mice were placed in a restrainer prior to obtaining plasma (isolated from blood obtained from the cut tail) and liver tissue.

Liver metabolic flux analysis

The metabolic model of liver metabolism, constructed using the INCA software tool (accessible at http://mfa.vueinnovations.com/mfa) (35), has been described in detail previously (34) and was developed with consideration to previously published models of liver intermediary metabolism (36–38). Assumptions and limitations of the flux analysis approach have been outlined in our prior publication (34). Plasma samples obtained ~2 h after the start of the [^{13}C$_3$]propionate infusion were divided into three aliquots for chemical conversion of glucose to its di-O-isopropylidene propionate, aldonitrile pentapropionate, and methyloxime pentapropionate derivatives. Following protein precipitation with cold acetone, plasma samples were derivatized as described in detail elsewhere (39). All derivatives were dissolved in ethyl acetate, transferred to glass inserts, and placed in GC injection vials for GC-MS analysis. GC-MS analysis was performed with an Agilent (Agilent Technologies, Santa Clara, CA) GC and MS system, using the protocol detailed previously (34). Briefly, derivatized samples were introduced to the column in splitless injection mode using helium as the carrier gas. The column was held at 80°C for 1 min, ramped to 280°C at 20°C/min (or 10°C/min for methyloxime pentapropionate) and held for 4min, and further increased to 325°C at 40°C/min. Following a 5 min solvent delay, MS data were collected in scan mode from m/z 300–320, m/z 100–500, and m/z 144–260 for di-O-isopropylidene propionate, aldonitrile pentapropionate, and methyloxime pentapropionate plasma glucose derivatives, respectively. MS peaks were integrated in MATLAB to yield mass isotopomer distributions (MIDs) for m/z 173–177, m/z 259–263, m/z 284–288, m/z 370–374 (aldonitrile pentapropionate),
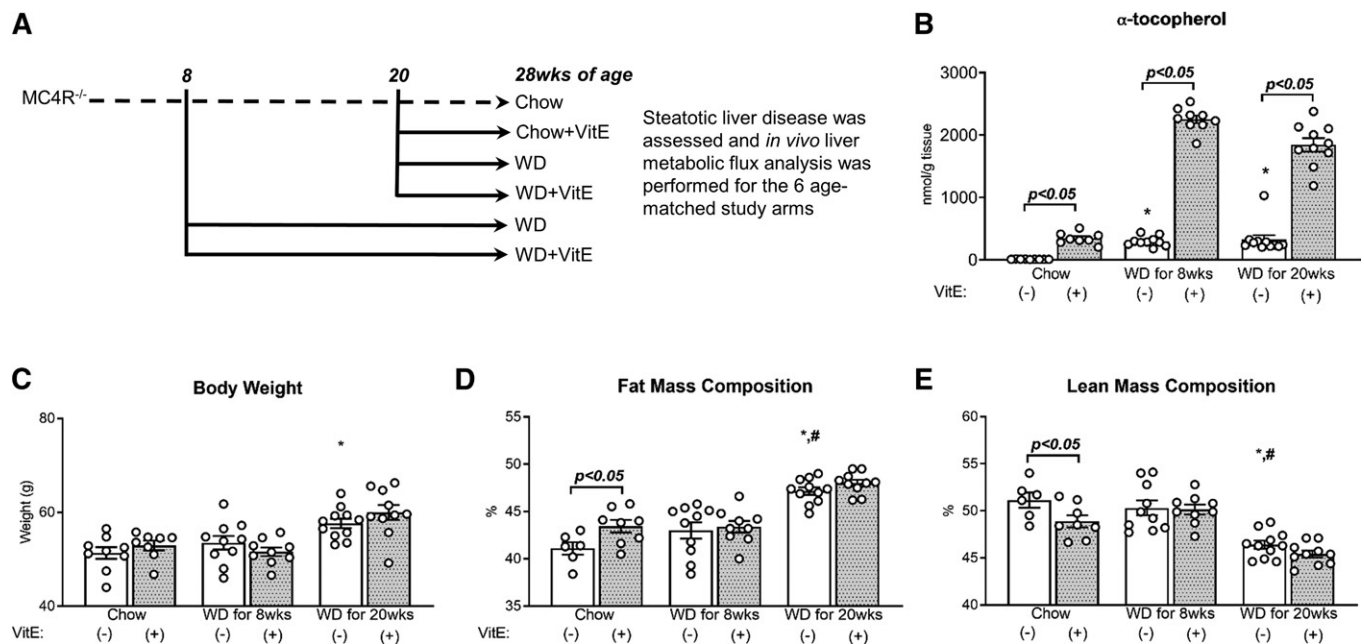
Fig. 1. Design of dietary intervention and its effects on body weight and composition. After weaning, mice were placed on a standard chow diet (A). At 8 weeks of age, mice were either maintained on chow or switched to WD (±VitE) for 20 weeks. One cohort of mice remained on chow until the end of the study; others were given chow+VitE or WD (±VitE) at 20 weeks of age for 8 weeks. All mice were 28 weeks of age upon completion of the study, when measurements of hepatic α-tocopherol (nanomoles per gram of tissue) (B), body weight (grams) (C), whole-body fat mass (percent) (D), and whole-body lean mass (percent) (E) were obtained. Data are presented as mean ± SEM (n = 6–10, shown as white circles). *P < 0.05 versus chow, #P < 0.05 versus WD for 8 weeks, VitE effects are indicated by brackets on each graph.

m/z 301–311 (di-*O*-isopropylidene propionate), and *m/z* 145–148 (methyloxime pentapropionate).

MIDs for these six plasma glucose fragment ions were regressed using INCA to estimate in vivo metabolic fluxes associated with CAC and glucose-producing pathways in the liver. After fixing citrate synthase flux (V_{CS}) to 100, relative fluxes were estimated by minimizing the sum of squared residuals between simulated and experimentally determined MIDs. Measurement errors were specified to be either 0.5 mol% or the SEM, whichever was greater. Best-fit flux estimates were obtained through least-squares regression using a minimum of 25 random initial parameter sets. Goodness of fit was assessed by a chi-square test, and 95% confidence intervals were calculated by evaluating the sensitivity of the best-fit sum of squared residual to variations in each flux value (40). Relative fluxes were converted to absolute fluxes using the known [6,6-^{2}H$_2$]glucose infusion rate and the measured weight of each mouse.

Plasma analyses, body composition, hepatic α-tocopherol, and liver lipids measurements

Plasma glucose concentrations were determined using an Accu-Chek glucometer (Roche, Risch-Rotkreuz, Switzerland). Plasma enzyme concentrations [alanine transaminase (ALT), aspartate transaminase (AST), lactate dehydrogenase (LDH), γ glutamyl transferase (GGT)], triglycerides, and cholesterol were measured using a VetAxcel chemistry analyzer equipped with a holographic diffraction grating spectrophotometer (Alfa Wassermann Diagnostic Technologies LLC, West Caldwell, NJ). Immunoreactive insulin was measured using a double-antibody method (41). Plasma NEFAs were measured using HR Series NEFA-HR(2) kit (FUJIFILM Wako Diagnostics USA Corporation, Richmond, VA). Plasma β-hydroxybutyrate (BHB) was measured using a BHB assay kit (ab83390) (Abcam, Cambridge, MA). Body composition was assessed using a Bruker Minispec benchtop pulsed NMR (7 T) system (model mq7.5) (Bruker, Billerica, MA). Hepatic α-tocopherol was measured as previously described (42). Briefly, a 10% homogenate was prepared in ice-cold PBS. An equal volume of ethanol containing an internal standard was added to each sample. Samples were mixed and extracted twice with five volumes of hexane, dried under a stream of nitrogen gas, resuspended in ethanol, and analyzed by UPLC equipped with an Aquity BEH C18 column (100 mm, 1.7 μm, 2.1 mm ID) and fluorescence detector (Waters Corporation, Milford, MA). Liver lipids were isolated in the chloroform phase obtained from Folch extraction, and lipid classes were separated with Silica Gel 60A plates developed in petroleum ether, diethyl ether, and acetic acid (80:20:1). Plates for ceramide analysis were rechromatographed in heptane, isopropyl ether, and acetic acid (60:40:3). Liver lipids were visualized with rhodamine 6G; phospholipids, ceramides, diglycerides, and triglycerides were scraped from plates, transmethylated with BF$_3$/methanol, and analyzed with an Agilent 7890 gas chromatograph (SP2380 column) and flame ionization detector (FID). The retention times of known standards were used to identify fatty acid methyl esters; quantification was achieved through a comparison to odd-chain fatty acids that were included as internal standards in the analysis.

Liver histology

Liver tissues were fixed in 10% neutral buffered formalin, routinely processed and embedded in paraffin, and cut into 5 μm sections for H&E and Sirius Red staining and F4/80 (NB600-404; Novus Biologicals LLC, Littleton, CO) immunohistochemistry. Microscopic evaluation and visual scoring were performed by veterinary pathologist K.L.B.; histological features were graded for steatosis, inflammation, ballooning, and fibrosis based on the classification algorithm described elsewhere (43). The activity score was calculated as the sum of the hepatocyte ballooning and lobular inflammation grades.

Analysis of mRNA expression

RNA was isolated from ∼30–50 mg of liver using the Direct-zol RNA MiniPrep kit (Genesee Scientific, San Diego, CA). cDNA was synthesized using the iScript cDNA synthesis kit (Bio-Rad, Hercules, CA). cDNA was diluted 1:2 and then used for quantitative real-time PCR analysis on a CFX96 cycler (Bio-Rad). TaqMan probes were purchased from the "Assays-on-Demand" program at Applied Biosystems (Foster City, CA). Gene expression was normalized to 18S using the $2^{-\Delta\Delta Ct}$ method.

Statistics

Unless otherwise specified, data are presented as means ± SEM. Differences between groups were tested using ANOVA and Tukey multiple comparisons post hoc analysis for WD effects. Two-tailed *t*-tests were performed to assess differences caused by VitE supplementation. Analysis of histological scoring was performed using Kruskall-Wallis ANOVA with a Dunn's multiple comparisons test for post hoc analysis; pairwise comparisons for VitE effects were performed using a Mann-Whitney test. Significant differences were defined at $P < 0.05$.

RESULTS

Overconsumption of WD exacerbated NASH severity

MC4R$^{-/-}$ mice fed a chow diet were ∼50 g with >40% body fat mass (Fig. 1C, D). Several chow-fed mice exhibited high levels of steatosis, lobular inflammation, hepatocyte ballooning, and activity (**Fig. 2A**, D–G), indicating severe liver disease; a fraction of chow-fed mice also exhibited elevated fibrosis (Fig. 2B, H). Greater than 10% of the liver (by mass) was composed of triglycerides (**Fig. 3A**). Eight weeks of WD had no impact on body weight or composition (Fig. 1C–E) but significantly increased plasma triglycerides, cholesterol, BHB (**Table 1**), and liver triglycerides (Fig. 3A). NASH severity was exacerbated by 8 weeks of WD feeding (Fig. 2A, D–G), as significant increases in pathological features of liver disease were observed. Immunostaining of F4/80+ macrophages increased significantly with 8 weeks of WD feeding (Fig. 2C, I), consistent with upregulation of F4/80 gene expression (Fig. 2J, *Adgre1*). Other markers of inflammation were also elevated (genes *Itgax*, *Tnfa*, *IL-10*, *Tgfb1*, and *Acta2*, and inflammation scoring) (Fig. 2E, J). Although fibrosis was not significantly elevated compared with chow-fed mice, fibrogenic (*Timp1* and *Col1a1*) and ECM degrading (*MMP2*) genes were increased with 8 weeks of WD (Fig. 2J). These results are consistent with increases in plasma markers associated with hepatic injury/disease (ALT, AST, LDH) caused by 8 weeks of WD feeding (Table 1). Plasma glucose concentrations after a 5 h fast were significantly lower than in chow-fed controls (Table 1), which contrasts with a prior study that reported no difference in blood glucose levels between MC4R$^{-/-}$ mice on chow versus WD when fed ad libitum (31).

Twenty weeks of WD feeding elicited several similar characteristics of whole-body and liver-specific metabolic dysregulation as 8 weeks of WD feeding. Twenty weeks of
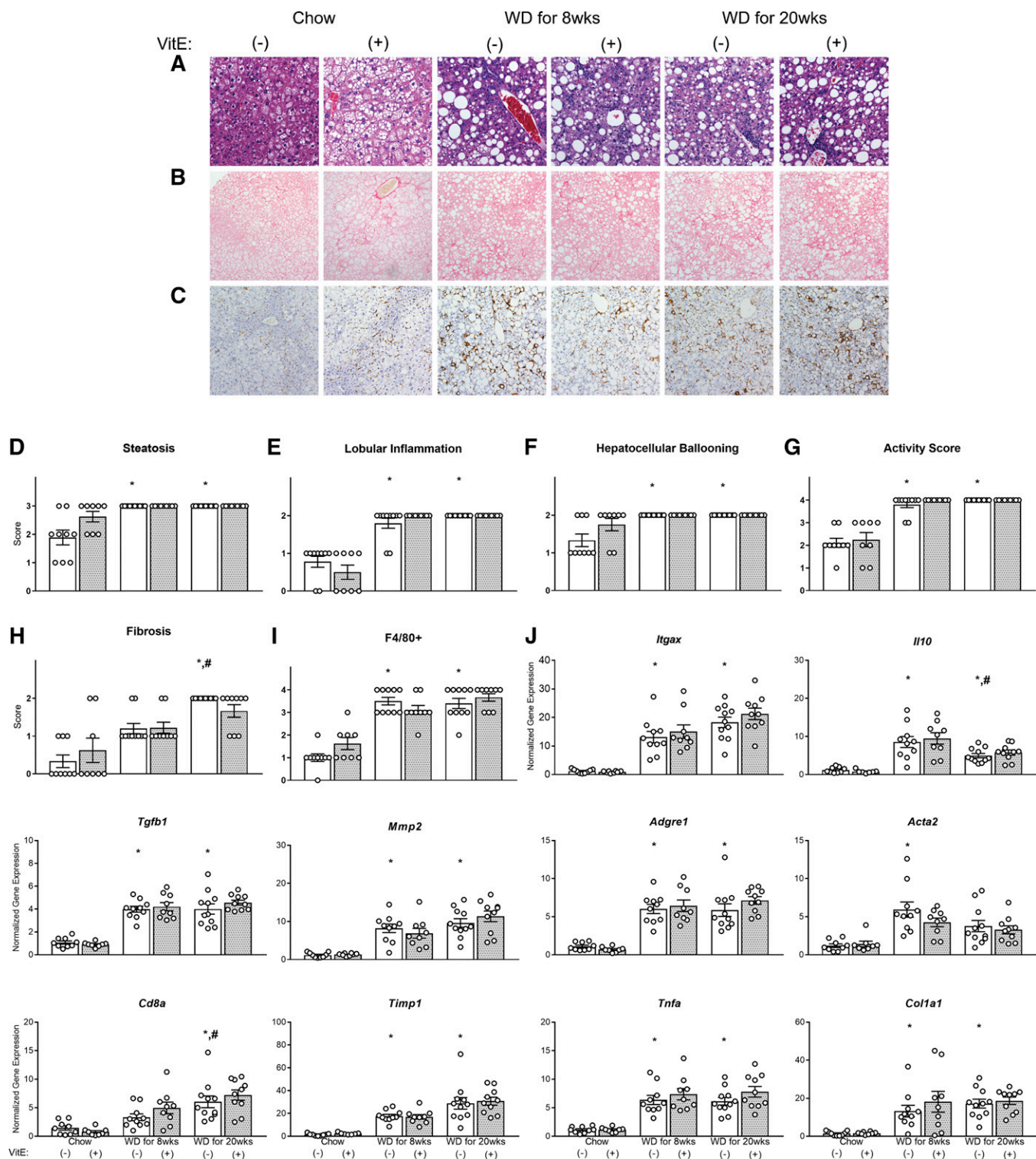
Fig. 2. Histology and gene expression in NASH development. Liver sections for 28-week-old mice fed chow, chow+VitE, WD for 8 weeks (±VitE), and WD for 20 weeks (±VitE) were stained with H&E (40× magnification) (A), picrosirius red (20× magnification) (B), or immunostained for F4/80+ cells (20× magnification) (C). Scoring of steatosis (D), lobular inflammation (E), hepatocellular ballooning (F), activity (G), fibrosis (H), and F4/80+ cell occupancy of the liver (I) (A scored for D–G, B for H, and C for I). mRNA expression of genes associated with inflammation and fibrogenesis (J). Values for each mouse (n = 7–11) are shown as white circles. *P < 0.05 versus chow, #P < 0.05 versus WD for 8 weeks.

WD resulted in significant gains in body weight and fat mass compared with both chow and 8 week WD groups (Fig. 1C, D). All mice fed WD for 20 weeks exhibited severe steatosis, lobular inflammation, hepatocellular ballooning, and overall activity (Fig. 2A, D–G); the severity of fibrosis was more pervasive with 20 weeks of WD feeding compared with 8 weeks of WD (Fig. 2B, H). Plasma biomarkers of liver damage (ALT, AST, LDH) and circulating triglycerides,
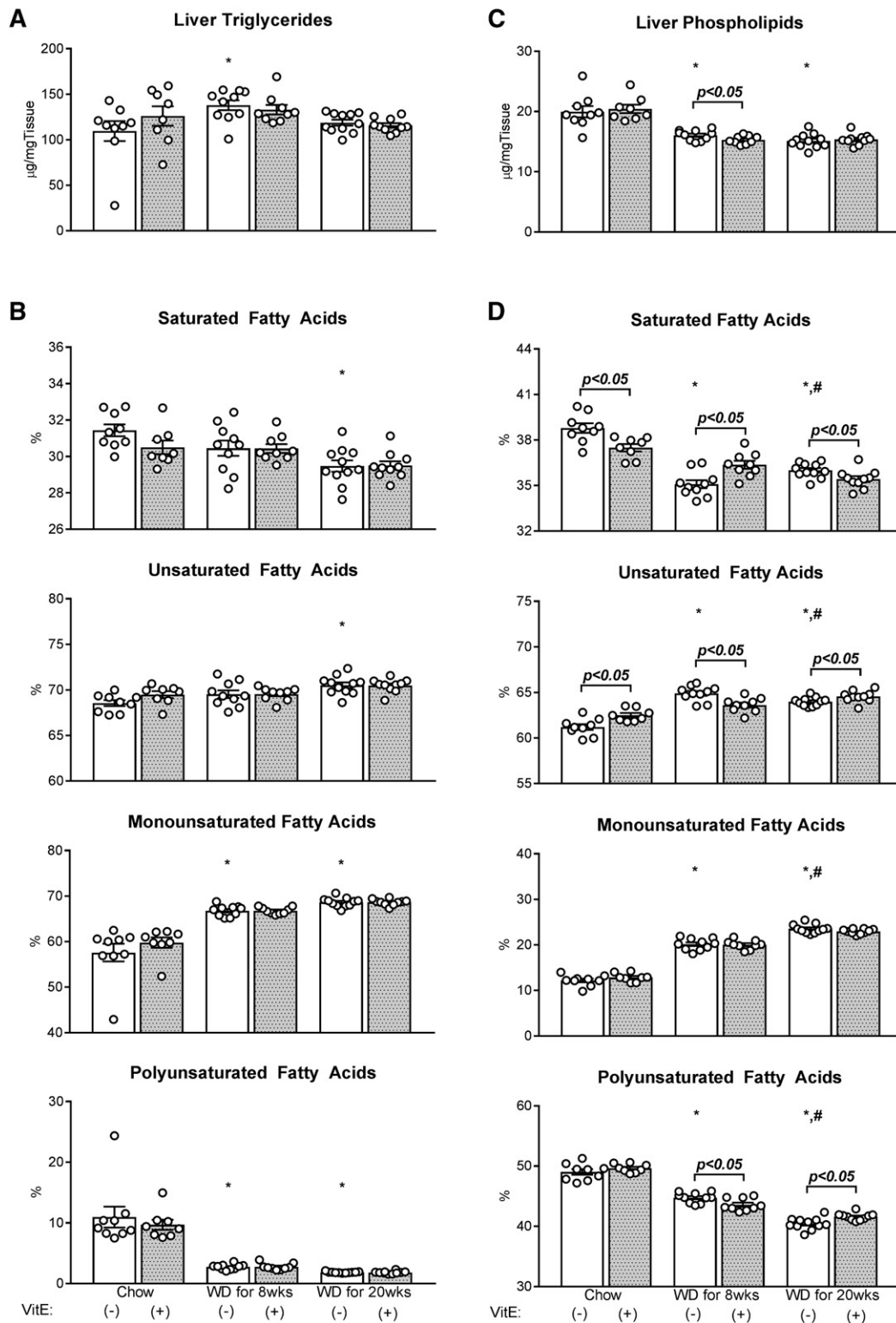
Fig. 3. Absolute liver triglycerides and phospholipids, and their saturation. Hepatic lipids [triglycerides (A, B) and phospholipids (C, D)] were measured using GC-FID and their composition calculated as the percentage contribution of saturated, monounsaturated, and polyunsaturated fatty acids to each lipid species. Data are presented as mean ± SEM (n = 8–11, shown as white circles). *$P < 0.05$ versus chow, #$P < 0.05$ versus WD for 8 weeks, VitE effects are indicated by brackets on each graph.

cholesterol, and BHB were similarly elevated, as observed in mice fed WD for 8 weeks (Table 1). Twenty weeks of WD feeding also increased the quantity of F4/80+ macrophages in the liver compared with chow-fed mice (Fig. 2C, I). With

the exception of an increase in *Cd8a* expression and decrease in *IL10* expression, 20 weeks of WD feeding led to similar effects on inflammatory and fibrogenic gene expression as 8 weeks of WD (Fig. 2J). Liver triglycerides (Fig. 3A)

TABLE 1. Circulating parameters in WD-mediated NASH and VitE treatment

	Chow		WD for 8 weeks		WD for 20 weeks	
VitE	(−)	(+)	(−)	(+)	(−)	(+)
ALT (U/l)	83.8 ± 14.3	140.5 ± 20.1^a	490.4 ± 51.8^b	579.8 ± 38.3	583.0 ± 40.3^b	575.2 ± 46.2
AST (U/l)	80.8 ± 12.5	113.8 ± 15.6	375.8 ± 40.0^b	446.0 ± 24.4	380.4 ± 36.2^b	463.4 ± 40.3
Chol (mg/dl)	142.5 ± 11.0	152.0 ± 11.4	426.0 ± 33.8^b	470.9 ± 14.0	484.8 ± 14.9^b	520.0 ± 15.3
TGs (mg/dl)	74.8 ± 2.6	78.5 ± 2.1	100.4 ± 3.5^b	106.0 ± 4.0	97.0 ± 3.7^b	87.8 ± 3.4
NEFA (mmol/l)	0.697 ± 0.079	0.784 ± 0.075	0.874 ± 0.053	0.868 ± 0.032	0.896 ± 0.021	0.836 ± 0.051
BHB (nmol/ml)	944.1 ± 87.0	1135 ± 140.4	2503 ± 132.0^b	2516 ± 241.5	2347 ± 274.5^b	2419 ± 86.0
GGT (U/l)	5.0 ± 0.8	5.0 ± 0.8	4.4 ± 0.4	3.1 ± 0.5	4.8 ± 0.9	4.4 ± 0.4
LDH (U/l)	336.0 ± 35.5	441.0 ± 56.3	1570.2 ± 291.6^b	1752.7 ± 279.4	2280.8 ± 371.1^b	2569.8 ± 219.8
Insulin (ng/ml)	7.5 ± 0.9	11.7 ± 1.6^a	6.7 ± 0.8	6.1 ± 0.6	5.0 ± 0.5	4.5 ± 0.5
Glucose (mg/dl)	162.3 ± 7.8	192.1 ± 8.6^a	137.3 ± 5.6^b	144.3 ± 3.9	136.2 ± 4.5^b	135.8 ± 4.9

Data are expressed as mean ± SEM, n = 8–11 mice. GGT, γ glutamyl transferase.
^{a}$P < 0.05$ versus no VitE treatment, same diet.
^{b}$P < 0.05$ versus chow.

and plasma glucose (Table 1) were equal to or lower than chow-fed mice, respectively, despite the exacerbation of NASH severity by 20 weeks of WD feeding. Plasma NEFA concentrations trended higher in WD-fed mice but were not significantly different from the levels observed in chow-fed mice. In summary, overconsumption of WD for 8 or 20 weeks exacerbated liver disease severity without inducing proportional changes in liver triglycerides, plasma NEFAs, or body composition.

WD consumption altered liver lipid composition

Although WD effects on total liver triglyceride content were inconsistent between 8 and 20 weeks, WD feeding induced uniform changes in the composition of liver lipids with increasing diet duration. Specifically, 8 weeks of WD feeding reduced the proportion of polyunsaturated fatty acids in liver triglycerides while increasing their monounsaturation (Fig. 3B). Both 8 and 20 weeks of WD feeding reduced a similar range of long and very long polyunsaturated fatty acids in liver triglycerides (**Table 2**). Despite the high saturated fat content of WD (∼65%, primarily palmitate), only a small increase in 14:0 was observed with 8 and 20 weeks of WD feeding; in contrast, other saturated fatty acids (i.e., 16:0 and 18:0) either remained unchanged or reduced. The relative abundance of 18:1ω7 and 16:1 monounsaturated fatty acids increased while 18:1ω9 remained stable. The composition of liver triglycerides following 8 and 20 weeks of WD feeding were similar, with the exception of a further elevation in 18:1ω7 with 20 weeks of WD feeding.

Both 8 and 20 weeks of WD feeding reduced liver phospholipids by roughly 20–25% (Fig. 3C). Phospholipid saturation and polyunsaturation were reduced in favor of monounsaturation (Fig. 3D). The composition of all monounsaturated fatty acids (16:1, 18:1ω7, and 18:1ω9) increased with 8 weeks of WD feeding (**Table 3**). Eight weeks of WD increased and reduced the proportion of 16:0 and 18:0 in liver phospholipids, respectively. The relative abundance of 18:2, 20:5, 22:5ω3, and 22:6 polyunsaturated fatty acids reduced and 20:4, 22:4ω6, and 22:5ω6 increased compared with chow-fed mice. Twenty weeks of WD feeding elicited similar directional changes on the fatty acid composition of liver phospholipids, but to a greater extent in many instances (Table 3). As a result, phospholipid saturation and monounsaturation were higher and polyunsaturation lower with 20 weeks of WD feeding compared with 8 weeks of WD (Fig. 3D).

TABLE 2. Hepatic triglyceride fatty acid composition in NASH and antioxidant treatment

	Chow		WD for 8 weeks		WD for 20 weeks	
VitE	(−)	(+)	(−)	(+)	(−)	(+)
14:0	0.60 ± 0.08	0.68 ± 0.02	1.10 ± 0.04^a	1.04 ± 0.02	1.02 ± 0.02^a	0.99 ± 0.03
16:0	28.80 ± 0.27	27.95 ± 0.35	27.84 ± 0.42	27.83 ± 0.22	26.98 ± 0.29^a	27.06 ± 0.23
16:1	4.24 ± 0.15	4.40 ± 0.19	6.21 ± 0.21^a	6.04 ± 0.17	6.29 ± 0.14^a	5.99 ± 0.22
18:0	2.04 ± 0.14	1.88 ± 0.04	1.52 ± 0.04^a	1.58 ± 0.02	1.48 ± 0.03^a	1.46 ± 0.03
18:1ω9	47.01 ± 1.59	48.70 ± 1.10	49.90 ± 0.48	49.71 ± 0.27	50.19 ± 0.47	50.94 ± 0.54
18:1ω7	6.35 ± 0.38	6.68 ± 0.33	10.68 ± 0.30^a	11.04 ± 0.14	12.17 ± 0.13^{a,b}	11.72 ± 0.30
18:2	8.13 ± 1.17	6.99 ± 0.39	2.64 ± 0.13^a	2.68 ± 0.13	1.85 ± 0.02^a	1.81 ± 0.05
18:3ω3	0.0 ± 0.0	0.25 ± 0.08^c	0.0 ± 0.0	0.0 ± 0.0	0.0 ± 0.0	0.0 ± 0.0
20:3ω6	0.24 ± 0.06	0.26 ± 0.06	0.04 ± 0.02^a	0.03 ± 0.03	0.0 ± 0.0^a	0.0 ± 0.0
20:4	0.29 ± 0.08	0.27 ± 0.09	0.04 ± 0.02^a	0.03 ± 0.03	0.02 ± 0.02^a	0.03 ± 0.03
20:5	0.0 ± 0.0	0.11 ± 0.08	0.02 ± 0.02	0.0 ± 0.0	0.0 ± 0.0	0.0 ± 0.0
22:4ω6	0.0 ± 0.0	0.02 ± 0.02	0.0 ± 0.0	0.0 ± 0.0	0.0 ± 0.0	0.0 ± 0.0
22:5ω3	0.56 ± 0.14	0.49 ± 0.06	0.0 ± 0.0^a	0.0 ± 0.0	0.0 ± 0.0^a	0.0 ± 0.0
22:6	1.74 ± 0.51	1.32 ± 0.15	0.02 ± 0.02^a	0.03 ± 0.03	0.0 ± 0.0^a	0.0 ± 0.0

Data are expressed as mean (percent of lipid composition) ± SEM, n = 8–11 mice.
^{a}$P < 0.05$ versus chow.
^{b}$P < 0.05$ versus WD for 8 weeks.
^{c}$P < 0.05$ versus no VitE treatment, same diet.

TABLE 3. Hepatic phospholipid fatty acid composition in NASH and antioxidant treatment

VitE	Chow		WD for 8 weeks		WD for 20 weeks	
	(−)	(+)	(−)	(+)	(−)	(+)
16:0	18.54 ± 0.32	18.10 ± 0.26	19.58 ± 0.16[a]	20.43 ± 0.25[b]	20.71 ± 0.10[a,c]	20.46 ± 0.09
16:1	0.70 ± 0.14	0.76 ± 0.03	1.55 ± 0.04[a]	1.45 ± 0.05	1.92 ± 0.06[a,c]	1.93 ± 0.06
18:0	20.25 ± 0.39	19.40 ± 0.30	15.51 ± 0.23[a]	15.94 ± 0.21	15.29 ± 0.11[a]	14.97 ± 0.22
18:1ω9	8.50 ± 0.27	9.13 ± 0.23	13.09 ± 0.19[a]	13.18 ± 0.19	15.14 ± 0.16[a,c]	14.75 ± 0.16
18:1ω7	2.98 ± 0.19	2.97 ± 0.12	5.51 ± 0.22[a]	5.41 ± 0.15	6.49 ± 0.12[a,c]	6.28 ± 0.15
18:2	11.39 ± 0.51	11.06 ± 0.29	7.61 ± 0.29[a]	8.05 ± 0.17	7.03 ± 0.09[a]	6.80 ± 0.14
20:3ω6	3.45 ± 0.19	3.65 ± 0.11	3.81 ± 0.10	4.00 ± 0.11	3.48 ± 0.06	3.47 ± 0.04
20:4	19.06 ± 0.53	17.29 ± 0.18[b]	20.86 ± 0.37[a]	20.07 ± 0.14	20.77 ± 0.26[a]	21.02 ± 0.17
20:5	0.92 ± 0.22	1.26 ± 0.08	0.17 ± 0.07[a]	0 ± 0[b]	0 ± 0[a]	0 ± 0
22:4ω6	0 ± 0	0 ± 0	0.54 ± 0.07[a]	0.26 ± 0.08[b]	0.26 ± 0.11	0.72 ± 0.02[b]
22:5ω6	0 ± 0	0.20 ± 0.10	1.37 ± 0.09[a]	1.42 ± 0.11	0.52 ± 0.22[c]	1.43 ± 0.03[b]
22:5ω3	0.37 ± 0.12	0.75 ± 0.02[b]	0 ± 0[a]	0 ± 0	0 ± 0[a]	0.05 ± 0.05
22:6	13.84 ± 0.29	15.43 ± 0.28[b]	10.40 ± 0.21[a]	9.79 ± 0.10[b]	8.39 ± 0.23[a,c]	8.11 ± 0.09

Data are expressed as mean (percent of lipid composition) ± SEM, n = 8–11 mice.
[a] $P < 0.05$ versus chow.
[b] $P < 0.05$ versus no VitE treatment, same diet.
[c] $P < 0.05$ versus WD for 8 weeks.

Although they comprise minor constituents of the total mass of cellular lipids, diglycerides and ceramides have been implicated as markers of incomplete fat oxidation that may contribute toward insulin resistance and lipotoxicity in the context of NAFLD (44). Both 8 and 20 weeks of WD feeding reduced total diglyceride content in the liver without corresponding changes in ceramide content (**Fig. 4A**, C). While the balance between saturated and unsaturated species was unchanged by WD feeding (Fig. 4B, D), there was a redistribution of species within these groups: 14:0 ceramides decreased while 18:0 ceramides increased (**Table 4**); 18:1ω9 diglycerides decreased while 16:1 and 18:1ω7 increased (**Table 5**). Furthermore, the relative abundance of polyunsaturated (18:2) diglyceride species significantly decreased in response to 8 or 20 weeks of WD (Table 5). In summary, overconsumption of WD by genetically obese MC4R$^{-/-}$ mice reduced liver phospholipid and diglyceride content and reduced the abundance of polyunsaturated fatty acids in triglycerides, diglycerides, and phospholipids.

VitE supplementation did not resolve NASH

Because oxidative stress has been implicated as a central feature of NAFLD, we hypothesized that dietary provision of VitE would attenuate many of the maladaptive features induced by steatotic liver disease. Although the VitE content of chow and WDs were similar (∼40 versus ∼50 IU/kg, respectively), basal α-tocopherol concentrations in the livers of WD-fed mice were higher than chow-fed mice (Fig. 1B), presumably because VitE is lipid soluble and relies on
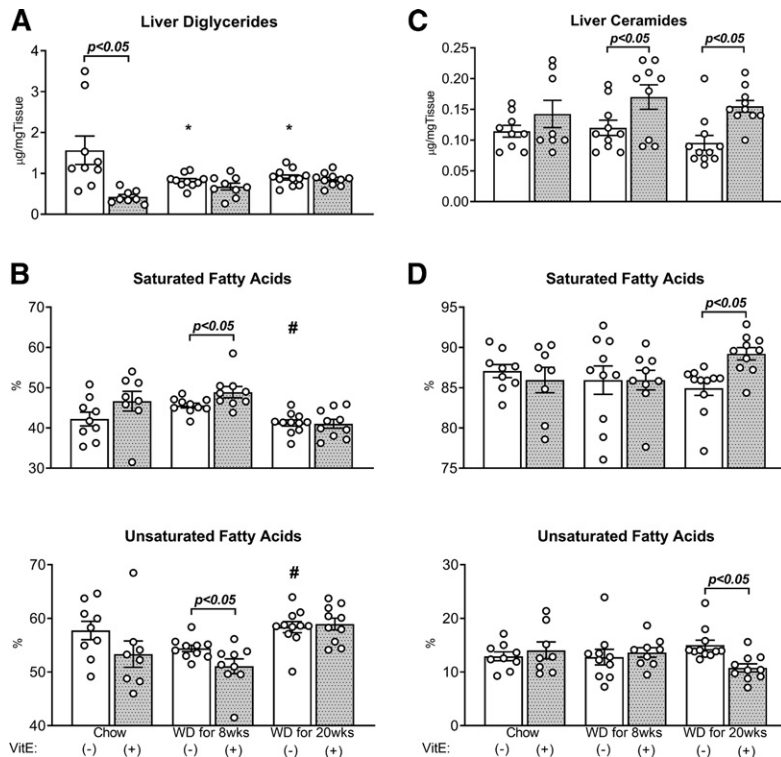
Fig. 4. Absolute liver diglycerides and ceramides, and their saturation. Hepatic lipids [diglycerides (A, B) and ceramides (C, D)] were measured using GC-FID and their composition calculated as the sum percent contribution of saturated and unsaturated fatty acids to lipid species. Data are presented as mean ± SEM (n = 8–11, shown as white circles). *$P < 0.05$ versus chow, #$P < 0.05$ versus WD for 8 weeks, VitE effects are shown on each graph.

TABLE 4. Hepatic ceramide fatty acid composition in NASH and antioxidant treatment

VitE	Chow		WD for 8 weeks		WD for 20 weeks	
	(−)	(+)	(−)	(+)	(−)	(+)
14:0	5.01 ± 0.35	3.00 ± 0.68	2.18 ± 0.64^a	4.25 ± 0.57	2.57 ± 0.52^a	5.14 ± 0.82
16:0	57.10 ± 1.56	53.55 ± 1.10	54.47 ± 1.89	53.26 ± 0.98	52.54 ± 1.45	57.79 ± 0.93^b
18:0	24.95 ± 1.30	29.41 ± 1.10^b	29.29 ± 1.32^a	28.44 ± 0.97	29.86 ± 0.66^a	26.28 ± 0.84^b
18:1ω9	12.93 ± 0.81	14.04 ± 1.56	12.78 ± 1.45	13.85 ± 0.89	15.04 ± 0.90	10.79 ± 0.76^b

Data are expressed as the mean (percent of lipid composition) ± SEM, n = 8–11 mice.
[a]$P < 0.05$ versus chow.
[b]$P < 0.05$ versus no VitE treatment, same diet.

pathways of fat absorption and chylomicron-associated transport for efficient delivery to the liver (45). In both diets, supplementation of VitE caused substantial increases in hepatic α-tocopherol concentrations. VitE supplementation of the chow diet produced a 32-fold increase in hepatic α-tocopherol, while mice fed WD+VitE for 8 or 20 weeks experienced an 8- or 6-fold increase in hepatic α-tocopherol content, respectively (Fig. 1B).

After 8 weeks of VitE treatment, fat mass increased and lean mass reduced in the chow+VitE group, with no differences in body weight (Fig. 1C–E). Contrary to our hypothesis, histological analysis did not reveal any significant difference in NASH scoring between chow- and chow+VitE-fed mice. Mice treated with VitE for 8 weeks exhibited equal steatosis, lobular inflammation, hepatocellular ballooning, activity, fibrosis, and F4/80+ staining as chow-fed controls (Fig. 2A–I). VitE supplementation elevated plasma ALT, insulin, and circulating glucose compared with the chow-fed controls (Table 1).

Supplementing WD with VitE did not lead to changes in body weight or composition in either 8 or 20 week cohorts (Fig. 1C–E). Histological assessment of the liver showed that VitE provision during WD-mediated NASH failed to mitigate inflammation, steatosis, ballooning, activity, fibrosis, or the presence of F4/80+ macrophages (Fig. 2A–I). VitE had no effect on inflammatory and fibrogenic gene expression in any cohort, consistent with histological descriptors (Fig. 2J). All measured plasma parameters were similar in mice fed WD+VitE for 8 and 20 weeks compared with mice fed WD alone (Table 1). In summary, VitE did not impact histological features of NASH in either chow- or WD-fed mice. Only during less severe steatotic liver disease

(chow-fed MC4R$^{-/-}$ mice) did VitE have an effect on other physiological parameters (i.e., body composition, circulating markers of liver function, blood glucose, and insulin concentrations). This effect could be attributable to differences in disease state induced by chow versus WD, or it could reflect the lower basal level of α-tocopherol in the livers of chow-fed mice and the larger fold change achieved after supplementing chow with VitE.

VitE supplementation exerted diet-dependent effects on liver phospholipid composition, but did not impact liver triglycerides

VitE had little effect on the quantity or composition of liver triglycerides when supplemented into either chow diet or WD (Fig. 3A, B; Table 2). Though absolute liver phospholipid content was similar (Fig. 3C), chow+VitE supplementation reduced hepatic phospholipid saturation (Fig. 3D). This result emanated exclusively from redistribution of polyunsaturated fatty acids (Table 3); provision of VitE reduced 20:4 and increased very long chain fatty acids 22:5ω3 and 22:6. However, VitE supplementation elicited inverse changes to liver phospholipids after 8 and 20 weeks of WD. WD+VitE for 8 weeks reduced total liver phospholipids compared with WD for 8 weeks, accompanied by a decrease in polyunsaturation and an increase in saturation (Fig. 3C, D). The increase in saturation was small but specific to 16:0, whereas 20:5, 22:4ω6, and 22:6 polyunsaturated fatty acids were all reduced (Table 3). The opposite occurred in mice fed WD+VitE for 20 weeks. Twenty weeks of VitE supplementation during WD feeding increased polyunsaturation and decreased saturation compared with WD for 20 weeks (Fig. 3C, D). Specific increases in 22:4 and

TABLE 5. Hepatic diglyceride fatty acid composition in NASH and antioxidant treatment

VitE	Chow		WD for 8 weeks		WD for 20 weeks	
	(−)	(+)	(−)	(+)	(−)	(+)
14:0	0.88 ± 0.08	0.88 ± 0.21	1.22 ± 0.04^a	1.51 ± 0.13^b	1.08 ± 0.06	1.07 ± 0.05
16:0	35.84 ± 1.18	36.20 ± 1.77	39.34 ± 0.58^a	39.87 ± 0.79	35.06 ± 0.80^c	35.40 ± 0.95
16:1	3.56 ± 0.20	3.80 ± 0.16	4.98 ± 0.15^a	4.66 ± 0.23	5.08 ± 0.17^a	4.62 ± 0.16
18:0	5.53 ± 0.52	9.58 ± 0.90^b	5.03 ± 0.41	7.55 ± 1.02^b	5.10 ± 0.91	4.58 ± 0.26
18:1ω9	44.57 ± 1.63	40.02 ± 2.36	37.57 ± 0.67^a	35.38 ± 1.13	39.57 ± 1.09^a	42.67 ± 1.37
18:1ω7	5.35 ± 0.56	5.56 ± 0.13	10.57 ± 0.24^a	9.10 ± 0.81	$12.65 \pm 0.41^{a,c}$	10.84 ± 0.27^b
18:2	4.28 ± 0.50	3.96 ± 0.40	1.28 ± 0.06^a	1.93 ± 0.60	1.08 ± 0.27^a	0.81 ± 0.10

Data are means (% of lipid composition) ± SEM, n = 8–11 mice.
[a]$P < 0.05$ versus chow.
[b]$P < 0.05$ versus no VitE treatment, same diet.
[c]$P < 0.05$ versus WD for 8 weeks.

22:5ω6 fatty acids were induced by the provision of VitE (Table 3). In summary, supplementation of dietary VitE had discordant effects on phospholipid composition that were dependent on the composition of the diet (chow versus Western) and the duration of WD feeding.

Supplementation of WD with VitE increased liver ceramide content and saturation

Supplementation of chow diet with VitE reduced liver diglyceride content (Fig. 4A) and increased the relative abundance of 18:0 species in both ceramides (Table 4) and diglycerides (Table 5), but without significantly perturbing their overall extent of saturation (Fig. 4B, D). In contrast, VitE supplementation of WD for 8 or 20 weeks induced significant elevations in liver ceramides (Fig. 3C), and 20 weeks of WD+VitE increased the saturation of liver ceramides in comparison to WD alone (Fig. 3D, Table 4). Although an increase in diglyceride saturation was observed by supplementing WD with VitE for 8 weeks, this effect was not seen in the 20 week WD groups (Fig. 4B, Table 5). In summary, VitE supplementation of WD increased the content of total liver ceramides and the relative abundance of some saturated diglyceride and ceramide species.

WD altered liver energy metabolism and glucose production

Simultaneous infusion of ^{2}H- and ^{13}C-enriched isotopes followed by model-based analysis of glucose enrichment enabled assessment of metabolic fluxes in conscious, unstressed mice. Endogenous glucose production (V_{EndoRa}) emanated predominantly from gluconeogenesis derived from CAC intermediates [gluconeogenesis from the citric acid cycle (V_{Enol})] in chow-fed mice following an ~20 h fast (**Fig. 5A**, D). Greater than 50% of the anaplerotic flux through pyruvate carboxylase (V_{PC}) and V_{PCK} reactions was condensed into glucose (V_{Enol}), with the remainder recycled through V_{PK+ME} (Fig. 5D–G). Total anaplerosis was ~2-fold the rate of the CAC (V_{CS}) (Fig. 5E, I). The increase in liver disease severity with 8 weeks of WD corresponded to accelerated flux through anaplerotic reactions (V_{PC} and V_{PCK}) (Fig. 5E, F). The increment in total anaplerotic fluxes did not result in an increase in glucose production or gluconeogenesis. Rather, the increment was balanced by an increase in the recycling of PEP to pyruvate (V_{PK+ME}) (Fig. 5G). It is noteworthy that NASH severity was exacerbated by 8 weeks of WD feeding, yet CAC activity (V_{CS}), glucose production, and body composition were not different from chow controls (Fig. 5I).

Twenty weeks of WD feeding increased glucose production above mice fed chow or WD for 8 weeks (Fig. 5A). The increase in glucose production resulted from an increase in glycogenolysis (V_{PYGL}) and V_{Enol} (Fig. 5B, D). Net (V_{LDH}) and total (V_{PCK}) anaplerosis were elevated above mice fed chow and WD for 8 weeks (Fig. 5E, H). Pyruvate cycling was further elevated by extending the duration of WD from 8 weeks to 20 weeks (Fig. 5E–G). In contrast to chow and 8 week WD groups, the rate of the CAC (V_{CS}) was also accelerated by 20 weeks of WD feeding (Fig. 5I). The ratio of gluconeogenesis to CAC activity (V_{Enol}/V_{CS}) remained ~1 in mice fed chow, WD for 8 weeks, or WD for 20 weeks. In summary, a diet high in sucrose, cholesterol, and saturated fat accelerated oxidative and glucose-producing metabolic fluxes in NASH; these features were intensified by extending the duration of WD feeding (**Fig. 6**).

VitE supplementation exacerbated WD-mediated effects on liver energy metabolism and glucose production
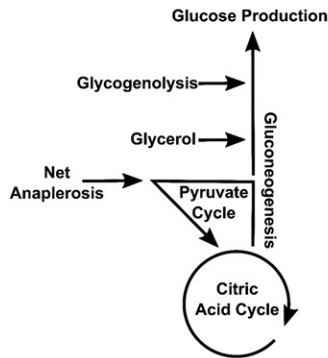
Mitochondrial metabolism is a major source of ROS; we hypothesized that the provision of VitE might limit the severity of steatotic liver disease and its associated metabolic phenotypes. In chow-fed mice, VitE supplementation reduced the rate of the CAC (V_{CS}) (Fig. 5I). No effects were observed on other glucose-producing or oxidative fluxes (Fig. 5A–H). The supplementation of VitE with WD feeding for 8 weeks accelerated V_{Enol} (Fig. 5D) and V_{EndoRa} (Fig. 5A). Glucose-producing fluxes were amplified alongside anaplerotic (V_{PCK}, V_{PC}, V_{LDH}), pyruvate cycling (V_{PK+ME}), and CAC (V_{CS}) fluxes (Fig. 5E–I). The trends in metabolism observed in mice fed WD+VitE for 8 weeks mirrored those of mice fed WD alone for 20 weeks. Supplementation of WD with VitE for 20 weeks failed to correct or exacerbate any WD-induced changes in liver metabolic fluxes (Figs. 5A–I, 6). Thus, metabolic phenotypes induced by WD feeding were not corrected by dietary supplementation of VitE; rather, VitE accelerated WD-induced metabolic dysregulation in the liver (Fig. 6).

DISCUSSION

Liver mitochondria coordinate substrate catabolism with anabolism to sustain the nutrient demands of extrahepatic tissues. In fasting, for example, the supply of acetyl-CoA for ketogenesis and CAC metabolism is sustained through β-oxidation and inhibition of de novo lipogenesis, which, in turn, support liver gluconeogenesis. Conditions that overload the liver with lipid, through overnutrition, exogenous infusion, ectopic redistribution, and/or de novo synthesis, distort mitochondrial morphology (46), function (2, 14, 47), and oxidative metabolic activity (2–4, 44). For these reasons, mitochondrial metabolism has been the focal point of recent investigations of NAFLD and NASH (2–4, 14, 44, 48). Satapati et al. (2) have rigorously delineated a time course for the development of NAFLD after 8, 16, and 32 weeks of high-fat feeding (HFF) in mice. Although 8 weeks of HFF increased liver triglycerides and decreased hepatic insulin sensitivity, acceleration of CAC metabolism and gluconeogenesis did not occur until 16 and 32 weeks. At 32 weeks, ketone turnover was blunted during fasting and less responsive to insulin; additionally, fatty acid-supported mitochondrial respiration was elevated. Some similarities in mitochondrial metabolism and function have been observed in obese humans with and without NAFLD (3, 14). In patients with NASH, however, the upregulation of respiration was lost and inefficiencies in ATP generation emerged (14).

Our work commenced at the intersection of the aforementioned studies. We assessed hepatic oxidative and glucose metabolism in a mouse model that recapitulates
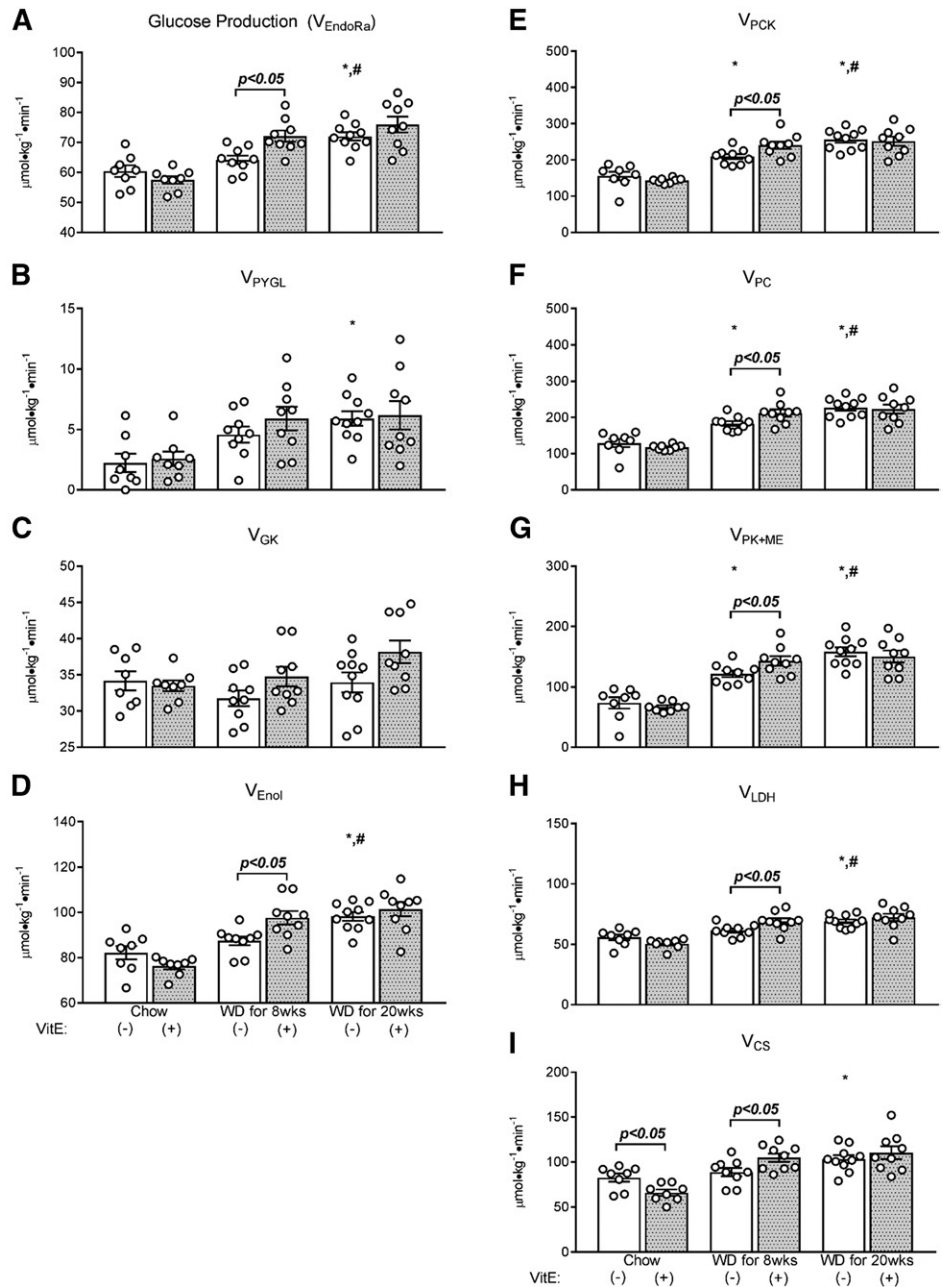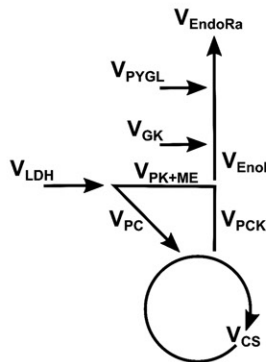
Fig. 5. In vivo glucose and mitochondrial oxidative metabolism in WD-mediated NASH and the effects of VitE treatment. Rates for enzyme-catalyzed reactions of the CAC, anaplerosis, cataplerosis, and glucose production (A–I) were estimated using metabolic flux analysis in 20 h-fasted mice fed chow, chow+VitE, WD for 8 weeks, WD+VitE for 8 weeks, WD for 20 weeks, and WD+VitE for 20 weeks. Individual fluxes were regressed using the enrichment of mass isotopomers of plasma glucose obtained from the artery of conscious, unstressed mice during the isotopic steady state. Data are presented as mean ± SEM (n = 8–10, shown as white circles). *$P < 0.05$ versus chow, #$P < 0.05$ versus WD for 8 weeks, VitE effects are indicated by brackets on each graph. V_{GK}, gluconeogenesis from glycerol.

several important characteristics of human NASH evoked by a diet high in saturated fat, sucrose, and cholesterol (30, 31). Chow-fed controls exhibited a baseline phenotype of elevated hepatic steatosis, ballooning, macrophage infiltration, and mild fibrosis. Even against this backdrop of steatotic liver disease, WD feeding for 8 or 20 weeks augmented NAFLD severity. The data presented by Koliaki et al. (14) imply that in vivo liver CAC activity may decrease during the progression to NASH. When situated in the murine in vivo milieu studied here, however, mitochondrial CAC metabolism exhibited flux adaptations similar to those observed during the progressive development of NAFLD (2) and high fructose *trans*-fat-induced NASH (44). Eight weeks of WD feeding accelerated anaplerosis and cataplerosis without altering gluconeogenesis or CAC activity, while 20 weeks of WD feeding further enhanced pyruvate cycling and accelerated glucose production, gluconeogenesis, and CAC activity. A progressive loss of coupling between substrate oxidation and respiratory ATP production may be responsible for the upward trend in CAC flux observed with increasing duration of WD feeding. An examination of liver mitochondrial function in the model applied
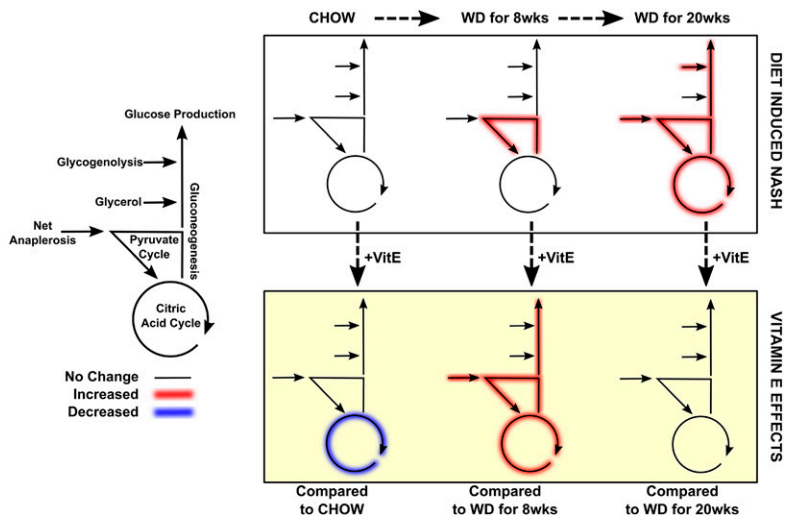
Fig. 6. The metabolic response of the liver to WD and VitE supplementation in NASH pathogenesis. The graphical representation summarizes the metabolic flux response of the liver to increasing WD-mediated liver disease. As NASH severity increased with WD duration (left to right, top rectangle), hepatic glucose and oxidative fluxes accelerated. Eight weeks of VitE treatment decreased CAC activity in mice fed chow (bottom rectangle). In contrast, 8 weeks of WD+VitE feeding accelerated glucose production and oxidative metabolism compared with 8 weeks of WD. Lastly, liver metabolic fluxes were identical in mice fed WD or WD+VitE for 20 weeks. These collective results illustrate the context-dependent response of liver intermediary metabolism to VitE treatment.

here would be useful for elucidating dichotomies in oxidative metabolism between ex vivo and in vivo settings.

The acceleration of hepatic glucose and oxidative metabolism in NASH observed here did not correlate directly with increased liver triglycerides. For example, absolute liver triglycerides were identical between chow-fed controls and mice fed WD for 20 weeks; yet, most liver glucose-producing and oxidative metabolic fluxes were heightened by 20 weeks of WD feeding. In contrast, liver triglycerides were elevated after 8 weeks of WD feeding when only pyruvate cycle fluxes increased. Perhaps the increased storage of lipid as triglycerides after 8 weeks of WD feeding protected against the augmentation of liver metabolism that occurred by extending WD to 20 weeks. WD feeding also significantly reduced liver phospholipids while increasing and decreasing their mono- and polyunsaturation, respectively. Liver phospholipid changes observed here are generally consistent with those previously observed in the ER of obese mice (22), where aberrant lipid metabolism has been shown to disrupt Ca^{2+} homeostasis and induce ER stress (22, 49). Significant changes to liver lipid saturation have also been reported in human NAFLD and NASH (50–53). Furthermore, recent research provides evidence for hormonal regulation of gluconeogenesis by ER Ca^{2+}-stimulated anaplerosis (54). Though speculative, it is plausible that liver lipid oversupply in NAFLD/NASH stimulates mitochondrial oxidative metabolism, anaplerosis, and gluconeogenesis through ER Ca^{2+}-dependent mechanisms that are responsive to changes in phospholipid composition. It would be informative to test the hypothesis that WD feeding impaired ER Ca^{2+} reuptake, which has been previously shown to promote apoptosis and CAC activity in hepatic cells exposed to excess palmitate (18–20).

Besides triglycerides and phospholipids, we also measured bioactive liver lipids relevant to the study of NAFLD/NASH [i.e., ceramides (44, 55, 56) and diglycerides (44, 57)]. In contrast to recent reports in another mouse model (44), no increases in total ceramides or diglycerides were observed in response to progressive worsening of diet-induced NASH. Several experimental differences may account for this apparent inconsistency. Ceramide and diglyceride measure-

ments here were normalized to tissue weight, as opposed to protein content (44). There were also significant differences in experimental design and mouse models. Simple steatosis and NASH were evoked previously using a high-*trans*-fat and high-fructose diet (TFD) (44). Wild-type mice were started on TFD or a control diet between 6 and 8 weeks of age and were maintained on the diet for 8 or 24 weeks; thus, comparisons were made between TFD-fed mice separated in age by ∼16 weeks (44). Mice studied here were age-matched, genetically obese (hyperphagic), and exhibited greater liver inflammation and fibrosis when fed a WD. To our knowledge, this study is the first to enable direct comparisons of in vivo liver metabolism across age-matched obese mice with differing grades of NASH severity.

In addition to quantifying the adaptive response of hepatic metabolism during WD-mediated NASH progression, we also examined the effects of VitE supplementation on fatty liver phenotypes. VitE is thought to suppress the effects of oxidative stress by interrupting peroxyl radical propagation across polyunsaturated fatty acids (23), and, thus, the effects of VitE supplementation in chow and WD feeding were antithetical to our hypotheses. We expected that increasing VitE content in all diet conditions would reduce the effects of oxidative stress and, thereby, lower inflammation and fibrosis. In mice fed a WD, VitE failed to reduce circulating ALT, AST, and LDH concentrations. Furthermore, descriptive features of WD-mediated steatosis, fibrosis, and inflammation were completely unaffected by VitE treatment in either 8 or 20 week groups. In fact, some indicators of metabolic dysfunction increased in mice fed a diet supplemented with VitE. Chow+VitE increased whole-body adiposity, reduced lean mass, and increased plasma ALT, blood glucose, and insulin concentrations compared with chow diet alone. Twenty weeks of WD+VitE increased the abundance and saturation of liver ceramides and 8 weeks of WD+VitE exacerbated metabolic flux dysregulation compared with WD alone. Prior studies have reported weight gain, increased plasma glucose, insulin, liver weight, and lipid content in mice gavaged biweekly with 150 mg VitE during 14 weeks of HFF (58). VitE supplementation also increased retroperitoneal adipocyte (rpWAT) hypertrophy

but lowered rpWAT weight and ROS markers (58). The authors suggested that VitE blunted adipocyte differentiation by reducing ROS during 14 weeks of HFF, which exacerbated the ectopic accumulation of lipids in the liver (58). After extending the regimen of VitE and HFF to 28 weeks, however, they found that VitE reduced liver lipid content, circulating insulin, triglycerides, and the HOMA index (59). The evidence presented here and elsewhere (27, 29, 58, 59) indicate that VitE may provide a benefit or a detriment during steatotic liver disease, depending on the context (i.e., the duration or severity of overnutrition and the dose or frequency of VitE administration).

Liver CAC oxidizes acetyl-CoA derived from substrate catabolism (60) to maintain the supply of NADH and flavin adenine dinucleotide hydroquinone ($FADH_2$) for the respiratory coupling of ATP production to oxygen consumption. Both energy-producing and -consuming fluxes were altered by VitE supplementation. In chow-fed mice, VitE lowered CAC flux, indicating an increase in cofactor reduction through alternative pathways (e.g., β-oxidation), lower ATP demands, and/or an increase in the efficiency of ATP-coupled respiration. In contrast, VitE supplementation for 8 weeks in the context of WD feeding accelerated CAC activity, pyruvate cycle fluxes, and hepatic glucose production from gluconeogenesis. These results indicate that antioxidant provision during NASH development may actually exacerbate the effects of insulin resistance on gluconeogenesis and increase the burden on the CAC for production of reduced cofactors. It is notable that liver phospholipid saturation was elevated and polyunsaturation reduced in mice fed WD+VitE for 8 weeks, without significant differences in body weight, composition, or liver triglycerides. Opposite effects on overall phospholipid saturation were observed with VitE supplementation of chow diet. The apparent correlation between VitE effects on phospholipid saturation and CAC flux provides further support for the hypothesis that changes in the composition of subcellular membranes may contribute to liver metabolic flux alterations during lipid overload (19, 61).

One limitation of our study design is that it did not attempt to directly assess the rate of synthesis or turnover of ketone bodies. Production of ketone bodies provides an alternative fate for mitochondrial acetyl-CoA derived from β-oxidation in the liver, and ketogenesis often increases during fasting or insulin resistance as a compensatory mechanism when the CAC has saturated the respiratory demand for NADH (2). We found that plasma BHB concentrations were significantly elevated in both 8 and 20 week WD-fed mice, but BHB levels were not impacted by VitE supplementation. Although we cannot rigorously assess whether the elevation in plasma BHB was due to increased ketogenesis or decreased clearance by peripheral tissues, prior studies have shown that increases in circulating ketone bodies in response to HFF are indicative of elevated turnover rates (2). Prior studies have also shown that fasting plasma ketones tend to eventually fall (relative to chow controls) after long-term HFF (2, 44), and this impairment of fasting ketogenesis may further exacerbate mitochondrial dysfunction in NASH. However, we did not observe a significant drop in fasting plasma BHB levels from 8 to 20 weeks of WD, suggesting that progression of NASH was not directly linked to impairment of fasting ketogenesis in our study. This inconsistency may reflect a number of differences in study design, including differences in animal models, age, diet composition, and fast duration. Nevertheless, assessing rates of ketone and fatty acid turnover would provide additional resolution for determining the fate of liver acetyl-CoA in NASH.

Another complication is that comparisons between chow-fed and WD-fed MCR4$^{-/-}$ mice may be confounded by metabolic discordance, rather than progression, of the NASH disease state under these two dietary regimes. It is possible that de novo lipogenesis, either in the liver or fat tissue, is a greater contributor to liver steatosis and whole-body adiposity in chow- versus WD-fed mice. We did not measure de novo lipogenesis or attempt to quantify its contribution to liver lipid content, so we could not assess whether hepatic lipid accumulation was derived from distinct sources under the two diets. Liver steatosis and whole-body adiposity were prevalent in both chow- and WD-fed animals, but the two diets had substantially different compositions based on caloric content (chow: 29% protein, 13% fat, 58% carbohydrate; WD: 17% protein, 40% fat, 43% carbohydrate). Furthermore, the manifestations of NASH observed in our studies may not be representative of the human condition and may be incongruent with other obese mouse models. For example, Chung et al. (62) achieved elevations in hepatic VitE concentrations that were similar to our study but reported protection against oxidative stress and inflammation in the livers of *ob/ob* mice with lipopolysaccharide-induced NASH. Our findings related to the nonprotective and, for certain indices, worsening effects of VitE treatment could be further bolstered by testing the same hypotheses in additional NASH models. It is likely that the duration and severity of NASH, the method of NASH induction, as well as the dose and frequency of VitE administration will impact the treatment response.

Overall, this study provided a quantitative assessment of in vivo liver metabolism in the progressive pathogenesis of diet-induced NASH and its treatment/prophylaxis with VitE. The success of some VitE therapies in patients with NAFLD and NASH offers hope for a facile solution to progressive steatotic liver disease (27). VitE is reported to not only reduce steatosis but also improve NASH in prior clinical studies (27). However, the most potent effects of VitE may involve modulation of inflammation and lipid storage in adipose tissue (58, 59), and its effectiveness in treating NAFLD could vary depending on the stage of disease progression (27, 29). Furthermore, our results suggest that the efficiency of VitE delivery to the liver may be strongly influenced by diet composition; this should be considered when comparing the effects of VitE provided with different diets, methods of administration, or dosing frequency. For example, Alcala et al. (58) provided comparatively larger quantities of VitE by oral gavage yet only observed ~3-fold changes in hepatic VitE concentration. At a minimum, the data presented in this study highlight the critical context-dependent nature of VitE supplementation. Numerous

dissimilarities between the human condition and murine models constrain the breadth of our conclusions. Nevertheless, our results suggest that use of VitE to treat NAFLD/NASH should be examined in a broader range of human patients and animal models to rigorously assess whether the proposed benefits outweigh the associated risks.⬛

REFERENCES

1. Koyama, Y., and D. A. Brenner. 2017. Liver inflammation and fibrosis. *J. Clin. Invest.* **127:** 55–64.
2. Satapati, S., N. E. Sunny, B. Kucejova, X. Fu, T. T. He, A. Méndez-Lucas, J. M. Shelton, J. C. Perales, J. D. Browning, and S. C. Burgess. 2012. Elevated TCA cycle function in the pathology of diet-induced hepatic insulin resistance and fatty liver. *J. Lipid Res.* **53:** 1080–1092.
3. Sunny, N. E., E. J. Parks, J. D. Browning, and S. C. Burgess. 2011. Excessive hepatic mitochondrial TCA cycle and gluconeogenesis in humans with nonalcoholic fatty liver disease. *Cell Metab.* **14:** 804–810.
4. Satapati, S., B. Kucejova, J. A. G. Duarte, J. A. Fletcher, L. Reynolds, N. E. Sunny, T. He, L. A. Nair, K. A. Livingston, X. Fu, et al. 2015. Mitochondrial metabolism mediates oxidative stress and inflammation in fatty liver. *J. Clin. Invest.* **125:** 4447–4462. [Erratum. 2016. *J. Clin. Invest.* 126: 1605.]
5. Keech, D. B., and M. F. Utter. 1963. Pyruvate carboxylase. II. Properties. *J. Biol. Chem.* **238:** 2609–2614.
6. Utter, M. F., and D. B. Keech. 1963. Pyruvate carboxylase. I. Nature of the reaction. *J. Biol. Chem.* **238:** 2603–2608.
7. Scrutton, M. C., and M. F. Utter. 1967. Pyruvate carboxylase. IX. Some properties of the activation by certain acyl derivatives of coenzyme A. *J. Biol. Chem.* **242:** 1723–1735.
8. Perry, R. J., J-P. G. Camporez, R. Kursawe, P. M. Titchenell, D. Zhang, C. J. Perry, M. J. Jurczak, A. Abudukadier, M. S. Han, X-M. Zhang, et al. 2015. Hepatic acetyl CoA links adipose tissue inflammation to hepatic insulin resistance and type 2 diabetes. *Cell.* **160:** 745–758.
9. Batenburg, J. J., and M. S. Olson. 1976. Regulation of pyruvate dehydrogenase by fatty acid in isolated rat liver mitochondria. *J. Biol. Chem.* **251:** 1364–1370.
10. Di Donato, L., C. Des Rosiers, J. A. Montgomery, F. David, M. Garneau, and H. Brunengraber. 1993. Rates of gluconeogenesis and citric acid cycle in perfused livers, assessed from the mass spectrometric assay of the 13C labeling pattern of glutamate. *J. Biol. Chem.* **268:** 4170–4180.
11. Szendroedi, J., M. Chmelik, A. I. Schmid, P. Nowotny, A. Brehm, M. Krssak, E. Moser, and M. Roden. 2009. Abnormal hepatic energy homeostasis in type 2 diabetes. *Hepatology.* **50:** 1079–1086.
12. Schmid, A. I., J. Szendroedi, M. Chmelik, M. Krssak, E. Moser, and M. Roden. 2011. Liver ATP synthesis is lower and relates to insulin sensitivity in patients with type 2 diabetes. *Diabetes Care.* **34:** 448–453.
13. Cortez-Pinto, H., J. Chatham, V. P. Chacko, C. Arnold, A. Rashid, and A. M. Diehl. 1999. Alterations in liver ATP homeostasis in human nonalcoholic steatohepatitis: a pilot study. *JAMA.* **282:** 1659–1664.
14. Koliaki, C., J. Szendroedi, K. Kaul, T. Jelenik, P. Nowotny, F. Jankowiak, C. Herder, M. Carstensen, M. Krausch, W. T. Knoefel, et al. 2015. Adaptation of hepatic mitochondrial function in humans with non-alcoholic fatty liver is lost in steatohepatitis. *Cell Metab.* **21:** 739–746.
15. Parks, E., H. Yki-Järvinen, and M. Hawkins. 2017. Out of the frying pan: dietary saturated fat influences nonalcoholic fatty liver disease. *J. Clin. Invest.* **127:** 454–456.
16. Nivala, A. M., L. Reese, M. Frye, C. L. Gentile, and M. J. Pagliassotti. 2013. Fatty acid-mediated endoplasmic reticulum stress in vivo: differential response to the infusion of soybean and lard oil in rats. *Metabolism.* **62:** 753–760.
17. Clore, J. N., J. S. Stillman, J. Li, S. J. D. O'Keefe, and J. R. Levy. 2004. Differential effect of saturated and polyunsaturated fatty acids on hepatic glucose metabolism in humans. *Am. J. Physiol. Endocrinol. Metab.* **287:** E358–E365.
18. Egnatchik, R. A., A. K. Leamy, Y. Noguchi, M. Shiota, and J. D. Young. 2014. Palmitate-induced activation of mitochondrial metabolism promotes oxidative stress and apoptosis in H4IIEC3 rat hepatocytes. *Metabolism.* **63:** 283–295.
19. Egnatchik, R. A., A. K. Leamy, D. A. Jacobson, M. Shiota, and J. D. Young. 2014. ER calcium release promotes mitochondrial dysfunction and hepatic cell lipotoxicity in response to palmitate overload. *Mol. Metab.* **3:** 544–553.
20. Egnatchik, R. A., A. K. Leamy, S. A. Sacco, Y. E. Cheah, M. Shiota, and J. D. Young. 2019. Glutamate-oxaloacetate transaminase activity promotes palmitate lipotoxicity in rat hepatocytes by enhancing anaplerosis and citric acid cycle flux. *J. Biol. Chem.* **294:** 3081–3090.
21. Leamy, A. K., C. M. Hasenour, R. A. Egnatchik, I. A. Trenary, C-H. Yao, G. J. Patti, M. Shiota, and J. D. Young. 2016. Knockdown of triglyceride synthesis does not enhance palmitate lipotoxicity or prevent oleate-mediated rescue in rat hepatocytes. *Biochim. Biophys. Acta.* **1861:** 1005–1014.
22. Fu, S., L. Yang, P. Li, O. Hofmann, L. Dicker, W. Hide, X. Lin, S. M. Watkins, A. R. Ivanov, and G. S. Hotamisligil. 2011. Aberrant lipid metabolism disrupts calcium homeostasis causing liver endoplasmic reticulum stress in obesity. *Nature.* **473:** 528–531.
23. Pacana, T., and A. J. Sanyal. 2012. Vitamin E and non-alcoholic fatty liver disease. *Curr. Opin. Clin. Nutr. Metab. Care.* **15:** 641–648.
24. Ni, Y., M. Nagashimada, F. Zhuge, L. Zhan, N. Nagata, A. Tsutsui, Y. Nakanuma, S. Kaneko, and T. Ota. 2015. Astaxanthin prevents and reverses diet-induced insulin resistance and steatohepatitis in mice: a comparison with vitamin E. *Sci. Rep.* **5:** 17192.
25. Nan, Y-M., W-J. Wu, N. Fu, B-L. Liang, R-Q. Wang, L-X. Li, S-X. Zhao, J-M. Zhao, and J. Yu. 2009. Antioxidants vitamin E and 1-aminobenzotriazole prevent experimental non-alcoholic steatohepatitis in mice. *Scand. J. Gastroenterol.* **44:** 1121–1131.
26. Raso, G. M., E. Esposito, A. Iacono, M. Pacilio, S. Cuzzocrea, R. B. Canani, A. Calignano, and R. Meli. 2009. Comparative therapeutic effects of metformin and vitamin E in a model of non-alcoholic steatohepatitis in the young rat. *Eur. J. Pharmacol.* **604:** 125–131.
27. Sanyal, A. J., N. Chalasani, K. V. Kowdley, A. McCullough, A. M. Diehl, N. M. Bass, B. A. Neuschwander-Tetri, J. E. Lavine, J. Tonascia, A. Unalp, et al. 2010. Pioglitazone, vitamin E, or placebo for nonalcoholic steatohepatitis. *N. Engl. J. Med.* **362:** 1675–1685.
28. Sanyal, A. J., P. S. Mofrad, M. J. Contos, C. Sargeant, V. A. Luketic, R. K. Sterling, R. T. Stravitz, M. L. Shiffman, J. Clore, and A. S. Mills. 2004. A pilot study of vitamin E versus vitamin E and pioglitazone for the treatment of nonalcoholic steatohepatitis. *Clin. Gastroenterol. Hepatol.* **2:** 1107–1115.
29. Bril, F., D. M. Biernacki, S. Kalavalapalli, R. Lomonaco, S. K. Subbarayan, J. Lai, F. Tio, A. Suman, B. K. Orsak, J. Hecht, et al. 2019. Role of vitamin E for nonalcoholic steatohepatitis in patients with type 2 diabetes: a randomized controlled trial. *Diabetes Care.* **42:** 1481–1488.
30. Itoh, M., T. Suganami, N. Nakagawa, M. Tanaka, Y. Yamamoto, Y. Kamei, S. Terai, I. Sakaida, and Y. Ogawa. 2011. Melanocortin 4 receptor-deficient mice as a novel mouse model of nonalcoholic steatohepatitis. *Am. J. Pathol.* **179:** 2454–2463.
31. Itoh, M., H. Kato, T. Suganami, K. Konuma, Y. Marumoto, S. Terai, H. Sakugawa, S. Kanai, M. Hamaguchi, T. Fukaishi, et al. 2013. Hepatic crown-like structure: a unique histological feature in non-alcoholic steatohepatitis in mice and humans. *PLoS One.* **8:** e82163.
32. Huszar, D., C. A. Lynch, V. Fairchild-Huntress, J. H. Dunmore, Q. Fang, L. R. Berkemeier, W. Gu, R. A. Kesterson, B. A. Boston, R. D. Cone, et al. 1997. Targeted disruption of the melanocortin-4 receptor results in obesity in mice. *Cell.* **88:** 131–141.
33. Ayala, J. E., D. P. Bracy, O. P. McGuinness, and D. H. Wasserman. 2006. Considerations in the design of hyperinsulinemic-euglycemic clamps in the conscious mouse. *Diabetes.* **55:** 390–397.
34. Hasenour, C. M., M. L. Wall, D. E. Ridley, C. C. Hughey, F. D. James, D. H. Wasserman, and J. D. Young. 2015. Mass spectrometry-based microassay of 2H and 13C plasma glucose labeling to quantify liver metabolic fluxes in vivo. *Am. J. Physiol. Endocrinol. Metab.* **309:** E191–E203.
35. Young, J. D. 2014. INCA: a computational platform for isotopically non-stationary metabolic flux analysis. *Bioinformatics.* **30:** 1333–1335.
36. Jones, J. G., R. Naidoo, A. D. Sherry, F. M. H. Jeffrey, G. L. Cottam, and C. R. Malloy. 1997. Measurement of gluconeogenesis and pyruvate recycling in the rat liver: a simple analysis of glucose and glutamate isotopomers during metabolism of [1,2,3-(13)C3]propionate. *FEBS Lett.* **412:** 131–137.
37. Katz, J. 1985. Determination of gluconeogenesis in vivo with 14C-labeled substrates. *Am. J. Physiol.* **248:** R391–R399.
38. Magnusson, I., W. C. Schumann, G. E. Bartsch, V. Chandramouli, K. Kumaran, J. Wahren, and B. R. Landau. 1991. Noninvasive tracing of Krebs cycle metabolism in liver. *J. Biol. Chem.* **266:** 6975–6984.

39. Antoniewicz, M. R., J. K. Kelleher, and G. Stephanopoulos. 2011. Measuring deuterium enrichment of glucose hydrogen atoms by gas chromatography/mass spectrometry. *Anal. Chem.* **83:** 3211–3216.

40. Antoniewicz, M. R., J. K. Kelleher, and G. Stephanopoulos. 2006. Determination of confidence intervals of metabolic fluxes estimated from stable isotope measurements. *Metab. Eng.* **8:** 324–337.

41. Morgan, C. R., and A. Lazarow. 1965. Immunoassay of pancreatic and plasma insulin following alloxan injection of rats. *Diabetes.* **14:** 669–671.

42. Clugston, R. D., H. Jiang, M. X. Lee, P. D. Berk, I. J. Goldberg, L. S. Huang, and W. S. Blaner. 2013. Altered hepatic retinyl ester concentration and acyl composition in response to alcohol consumption. *Biochim. Biophys. Acta.* **1831:** 1276–1286.

43. Bedossa, P., FLIP Pathology Consortium. 2014. Utility and appropriateness of the fatty liver inhibition of progression (FLIP) algorithm and steatosis, activity, and fibrosis (SAF) score in the evaluation of biopsies of nonalcoholic fatty liver disease. *Hepatology.* **60:** 565–575.

44. Patterson, R. E., S. Kalavalapalli, C. M. Williams, M. Nautiyal, J. T. Mathew, J. Martinez, M. K. Reinhard, D. J. McDougall, J. R. Rocca, R. A. Yost, et al. 2016. Lipotoxicity in steatohepatitis occurs despite an increase in tricarboxylic acid cycle activity. *Am. J. Physiol. Endocrinol. Metab.* **310:** E484–E494.

45. Kayden, H. J., and M. G. Traber. 1993. Absorption, lipoprotein transport, and regulation of plasma concentrations of vitamin E in humans. *J. Lipid Res.* **34:** 343–358.

46. Sanyal, A. J., C. Campbell-Sargent, F. Mirshahi, W. B. Rizzo, M. J. Contos, R. K. Sterling, V. A. Luketic, M. L. Shiffman, and J. N. Clore. 2001. Nonalcoholic steatohepatitis: association of insulin resistance and mitochondrial abnormalities. *Gastroenterology.* **120:** 1183–1192.

47. Pérez-Carreras, M., P. Del Hoyo, M. A. Martín, J. C. Rubio, A. Martín, G. Castellano, F. Colina, J. Arenas, and J. A. Solis-Herruzo. 2003. Defective hepatic mitochondrial respiratory chain in patients with nonalcoholic steatohepatitis. *Hepatology.* **38:** 999–1007.

48. Kalavalapalli, S., F. Bril, J. P. Koelmel, K. Abdo, J. Guingab, P. Andrews, W-Y. Li, D. Jose, R. A. Yost, R. F. Frye, et al. 2018. Pioglitazone improves hepatic mitochondrial function in a mouse model of nonalcoholic steatohepatitis. *Am. J. Physiol. Endocrinol. Metab.* **315:** E163–E173.

49. Park, S. W., Y. Zhou, J. Lee, J. Lee, and U. Ozcan. 2010. Sarco(endo) plasmic reticulum Ca2+-ATPase 2b is a major regulator of endoplasmic reticulum stress and glucose homeostasis in obesity. *Proc. Natl. Acad. Sci. USA.* **107:** 19320–19325.

50. Videla, L. A., R. Rodrigo, J. Araya, and J. Poniachik. 2004. Oxidative stress and depletion of hepatic long-chain polyunsaturated fatty acids may contribute to nonalcoholic fatty liver disease. *Free Radic. Biol. Med.* **37:** 1499–1507.

51. Araya, J., R. Rodrigo, L. A. Videla, L. Thielemann, M. Orellana, P. Pettinelli, and J. Poniachik. 2004. Increase in long-chain polyunsaturated fatty acid n - 6/n - 3 ratio in relation to hepatic steatosis in patients with non-alcoholic fatty liver disease. *Clin. Sci. (Lond.).* **106:** 635–643.

52. Arendt, B. M., E. M. Comelli, D. W. L. Ma, W. Lou, A. Teterina, T. Kim, S. K. Fung, D. K. H. Wong, I. McGilvray, S. E. Fischer, et al. 2015. Altered hepatic gene expression in nonalcoholic fatty liver disease is associated with lower hepatic n-3 and n-6 polyunsaturated fatty acids. *Hepatology.* **61:** 1565–1578.

53. Chiappini, F., A. Coilly, H. Kadar, P. Gual, A. Tran, C. Desterke, D. Samuel, J-C. Duclos-Vallée, D. Touboul, J. Bertrand-Michel, et al. 2017. Metabolism dysregulation induces a specific lipid signature of nonalcoholic steatohepatitis in patients. *Sci. Rep.* **7:** 46658.

54. Miller, R. A., Y. Shi, W. Lu, D. A. Pirman, A. Jatkar, M. Blatnik, H. Wu, C. Cárdenas, M. Wan, J. K. Foskett, et al. 2018. Targeting hepatic glutaminase activity to ameliorate hyperglycemia. *Nat. Med.* **24:** 518–524.

55. Holland, W. L., B. T. Bikman, L. P. Wang, G. Yuguang, K. M. Sargent, S. Bulchand, T. A. Knotts, G. Shui, D. J. Clegg, M. R. Wenk, et al. 2011. Lipid-induced insulin resistance mediated by the pro-inflammatory receptor TLR4 requires saturated fatty acid-induced ceramide biosynthesis in mice. *J. Clin. Invest.* **121:** 1858–1870.

56. Pagadala, M., T. Kasumov, A. J. McCullough, N. N. Zein, and J. P. Kirwan. 2012. Role of ceramides in nonalcoholic fatty liver disease. *Trends Endocrinol. Metab.* **23:** 365–371.

57. Finck, B. N., and A. M. Hall. 2015. Does diacylglycerol accumulation in fatty liver disease cause hepatic insulin resistance? *BioMed Res. Int.* **2015:** 104132.

58. Alcala, M., M. Calderon-Dominguez, D. Serra, L. Herrero, M. P. Ramos, and M. Viana. 2017. Short-term vitamin E treatment impairs reactive oxygen species signaling required for adipose tissue expansion, resulting in fatty liver and insulin resistance in obese mice. *PLoS One.* **12:** e0186579.

59. Alcalá, M., I. Sánchez-Vera, J. Sevillano, L. Herrero, D. Serra, M. P. Ramos, and M. Viana. 2015. Vitamin E reduces adipose tissue fibrosis, inflammation, and oxidative stress and improves metabolic profile in obesity. *Obesity (Silver Spring).* **23:** 1598–1606.

60. Owen, O. E., S. C. Kalhan, and R. W. Hanson. 2002. The key role of anaplerosis and cataplerosis for citric acid cycle function. *J. Biol. Chem.* **277:** 30409–30412.

61. Leamy, A. K., R. A. Egnatchik, and J. D. Young. 2013. Molecular mechanisms and the role of saturated fatty acids in the progression of non-alcoholic fatty liver disease. *Prog. Lipid Res.* **52:** 165–174.

62. Chung, M. Y., S. F. Yeung, H. J. Park, J. S. Volek, and R. S. Bruno. 2010. Dietary α- and γ-tocopherol supplementation attenuates lipopolysaccharide-induced oxidative stress and inflammatory-related responses in an obese mouse model of nonalcoholic steatohepatitis. *J. Nutr. Biochem.* **21:** 1200–1206.